Magnetic circular dichroism study of the selenium-substituted form (Fe_3Se_4) of bovine heart aconitase

Jacques L. BRETON,*§ Jacqueline A. FARRAR,* Mary Claire KENNEDY,† Helmut BEINERT‡ and Andrew J. THOMSON*

*Centre for Metalloprotein Spectroscopy and Biology, School of Chemical Sciences, University of East Anglia, Norwich NR4 7TJ, U.K.,
†Department of Biochemistry and Biophysics Research Institute, Medical College of Wisconsin, Milwaukee, WI 53226, U.S.A.,
and ‡Institute for Enzyme Research, University of Wisconsin, Madison, WI 53705–4098, U.S.A.

The selenium-substituted inactive form of mitochondrial aconitase contains one [3Fe-4Se]$^{1+/0}$ cluster [Surerus, Kennedy, Beinert and Münck (1989) Proc. Natl. Acad. Sci. U.S.A. **87**, 9846–9850]. This cluster was studied in both oxidized and reduced states by magnetic CD (MCD) and EPR spectroscopy. In the MCD spectra, intensity and transition wavelength shifts are observed when compared with the spectra of the native [3Fe-4S]$^{1+/0}$ cluster. These changes are used to differentiate between the charge-transfer transitions originating from inorganic and cysteinyl sulphur. Using also the data from the EPR spectra, the spin ground state is assigned as S = 1/2 for the oxidized [3Fe-4Se]$^{1+}$ cluster and S = 2 for the reduced [3Fe-4Se]^{0} cluster.

INTRODUCTION

Since the identification in the early 1980s of the [3Fe-4S]$^{1+/0}$ cluster, a significant amount of spectroscopic work {notably using Mössbauer [1–3], EPR [1–5], magnetic CD (MCD) [6], magnetic susceptibility [7] and Resonance Raman [8–10] techniques} has been undertaken to try to unravel the electronic structure of this cluster. It is now established that in the [3Fe-4S]$^{1+}$ oxidized state, the three iron atoms are high-spin ferric and antiferromagnetically coupled to give a resulting cluster spin ground state of S = 1/2 [2,11]. In the reduced state, [3Fe-4S]^{0}, the overall spin of the cluster is S = 2 with the iron valences being inequivalent at the cryogenic temperatures required for these techniques. However, despite these efforts there are still no satisfactory theoretical models which allow the assignment of the MCD transitions in the otherwise very characteristic MCD spectra of the [3Fe-4S]$^{1+/0}$ cluster.

In order to try to overcome similar difficulties, the inorganic acid-labile sulphide ions in [4Fe-4S] ferredoxins were replaced with selenium [12,13]. Selenium is a group-VIA third-row element, with chemical properties broadly similar to sulphur [13–15]. It was possible to reconstitute a [4Fe-4Se] cluster in place of the original [4Fe-4S] cluster, once the apoprotein had been prepared. These substitution experiments were inspired by the work of Rabinowitz and co-workers on ferredoxin cluster reconstitution [16,17]. Chemical and spectroscopic studies of these early selenium analogues gave a wealth of information. It was established for example from the hyperfine structure appearing in the EPR on ^{77}Se substitution in adrenodoxin that two inorganic chalcogenides were present per 2Fe cluster [18]. Spectroscopic assignments of the 330, 420 and 460 nm absorption peaks in the uv/visible spectrum of the [2Fe-2S]$^{2+}$ cluster were also made possible as these peaks were 'red shifted' (bathochromic shifts) by 5, 20 and 20 nm respectively on selenium substitution. This implies a greater inorganic chalcogenide S(e) character for the two lower-energy charge-transfer transitions, whereas the 330 nm band has therefore greater cysteinyl (S) character [12,13]. More generally, replacement of the inorganic sulphur by selenium in Fe/S clusters has the effect of decreasing ligand-to-metal charge-transfer energies [19,20].

The selenium-substitution techniques have since been applied to [4Fe-4S] clusters ([21] and references therein), as well as to [3Fe-4S] clusters [22]. The selenium derivatives are generally more labile than their sulphur counterparts [21], probably because of a less efficient folding of the polypeptide around the cluster, as Se is slightly larger than S [difference in covalent radius $\approx$ 1.3 nm (0.13 Å)]. X-ray-crystallographic studies on $[Fe_2Se_2(SR)_4]^{2-}$ and $[Fe_4Se_4(SR)_4]^{2-/3-}$ model compounds revealed geometries essentially similar to the sulphur-containing clusters [19,20], although the Fe-Se distance was longer than the Fe-S distance by 0.11 Å (van der Waals volume is increased by 25%). Selenium (mass atomic number 79) is more than twice as heavy as sulphur (mass atomic number 32) and therefore has a considerable effect on the vibrational properties of the substituted clusters. Resonance Raman spectroscopists used this property to compare and assign the observed vibrational modes for 2Fe [15] and 4Fe [21] clusters. Finally, the isotope ^{77}Se has a nuclear spin $I = 1/2$, which is very useful for studying ligand hyperfine interactions by EPR [18,23] and electron nuclear double-beam resonance in principle (although it has never been observed), as well as by NMR, particularly for assigning the β-cysteinyl protons [21]. Moreover, ^{77}Se NMR is also feasible [24].

The work of Meyer et al. [21] on *Clostridium pasteurianum* ferredoxin combined all these techniques to study the first reconstituted [4Fe-4Se] cluster. A mixture of high-spin ground states S = 1/2, 3/2 and 7/2 in the reduced [4Fe-4Se]$^{1+}$ state were identified for the first time, before a series of observations of spin states greater than 1/2, in native iron-sulphur proteins (*Azotobacter vinelandii* nitrogenase Fe protein [25–27], *Delsulfovibrio africanus* ferredoxin III [28], *Pyrococcus furiosus* ferredoxin [29] and *Bacillus subtilis* phosphoribosylpyrophosphate amidotransferase [30]) as well as for tetranuclear cluster analogues [31]. Analysis of the structure/spin states relationship of a series of model [4Fe-4S(e)]$^{1+}$ clusters has shown that ground-state vari-

Abbreviation used: MCD, magnetic circular dichroism.

§ To whom correspondence should be addressed.

ability was the general rule rather than the exception for these clusters, and that this property was extremely sensitive to external factors such as the terminal ligands [31]. In protein-bound [4Fe-4S(e)] clusters, constraints imposed by the polypeptide folding will therefore be the dominant factor. These experiments also confirmed the all-or-none character of the mechanism of *in vitro* iron-sulphur reconstitution.

MCD spectra of the two-[4Fe-4Se] cluster *C. pasteurianum* ferredoxin and the single-cluster *Bacillus stearothermophilus* ferredoxin have been reported [32]. In the case of *C. pasteurianum* ferredoxin the presence of a physical mixture of spin $S = 1/2$, $S = 3/2$ and $S = 7/2$ ground states for the reduced cluster prevented a thorough analysis of the magnetization properties. However, it was possible to recognize band shifts for the oxidized diamagnetic cluster as most transitions underwent bathochromic shifts of 30–60 nm, as expected. The picture was not as clear for the reduced cluster, mainly because of overlapping transitions, but in both cases a large increase in MCD intensity was observed (the absorption coefficients are three to four times those of the native sulphur clusters). This was explained in terms of the larger spin–orbit coupling constant for selenium (1700 cm^{-1}) than that for sulphur (380 cm^{-1}).

Only one case of selenium substitution of the [3Fe-4S] cluster has been reported so far, for bovine heart mitochondrial aconitase [22]. Mössbauer and EPR spectra of the oxidized cluster, as well as Mössbauer spectra of the reduced cluster, were presented. In the present paper we report the EPR and MCD spectra of the [3Fe-4Se] cluster substituted in bovine heart mitochondrial aconitase in the oxidized (+1) and reduced (0) oxidation states.

EXPERIMENTAL

Samples of [3Fe-4Se] selenium derivatives of bovine mitochondrial heart aconitase were prepared as previously described [22,33,34]. The apoenzyme was obtained by oxidative degradation of the Fe-S cluster with potassium ferricyanide, and subsequent cyanolysis to remove all inorganic sulphur. It was noticed in similar experiments [33] that S^{2-} was preserved as S^0 in cystine trisulphide and tetrasulphides bridges in the apoprotein if cyanolysis was not performed, thus preventing the reconstitution of a homogeneous [3Fe-4Se] cluster. Apoprotein prepared by this method can be reconstituted into holoaconitase with a good yield using substoichiometric amounts of Fe^{2+} and Se^{2-} ions. The inactive [3Fe-4Se] enzyme was then obtained by carefully titrating the active [4Fe-4Se] enzyme with potassium ferricyanide until less than 5% of the original activity remained [22,33]. Despite all these precautions, adventitious selenium was still bound to the protein, probably originating from breakdown of the [3Fe-4Se] cluster during the oxidation step, reflecting the higher lability of the selenium cluster than its sulphur counterpart. Similar results were obtained with persulphate as the oxidative agent.

A preparation of 390 μM $[3Fe\text{-}4Se]^{1+}$ cluster in 0.1 M Hepes buffer, pH 7.5, was used. Some 300 μl of the protein sample was mixed with 310 μl of ethanediol (51%, v/v), which was then divided into two 300 μl aliquots for MCD and EPR spectroscopy of the oxidized cluster. The cluster concentration was calculated to be 190 μM after the dilution with ethanediol. No attempt was made to measure the UV/visible spectrum to avoid unwanted exposure to air.

To produce the reduced $[3Fe\text{-}4Se]^0$ cluster, EDTA was first added to five times the molar concentration of the cluster (5 μl of a 116 mM EDTA stock solution to 570 μl of aconitase sample) to prevent cluster conversion on reduction. Then the sample was reduced with a four times molar excess of buffered dithionite (pH 7.6) over cluster. The final cluster concentration was 170 μM.

All sample manipulations were performed in an anaerobic glovebox (Faircrest, Croydon, Surrey, U.K.) under a nitrogen atmosphere ($O_2 < 2$ p.p.m.).

EPR spectra were recorded on an updated X-band Bruker ER200D SRC spectrometer equipped with an Oxford instruments ESR-900 helium flow cryostat. Spin densities of paramagnetic samples were estimated from integration of EPR spectra by comparison with a 1 mM Cu(II)/EDTA standard [35]. Low-temperature MCD spectroscopy was performed using a modified Jasco J-500D dichrograph and an Oxford instruments SM4 split-coil superconducting magnet. Procedures for measuring MCD spectra have been described elsewhere [36].

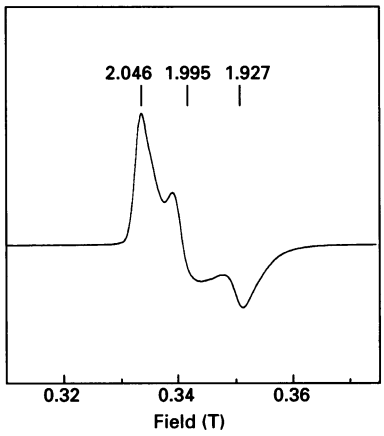

Figure 1 X-band EPR spectrum of $[3Fe\text{-}4Se]^{1+}$ seleno-aconitase from bovine heart

The concentration of $[3Fe\text{-}4Se]^{1+}$ clusters was 190 μM in 50% (v/v) ethanediol/0.1 M Hepes, pH 7.5. Experimental conditions were: microwave power = 2 mW; modulation amplitude = 5 G; temperature = 10 K; gain = 4×10^4. All concentrations are quoted after dilution. Effective g-values are indicated on the spectrum.

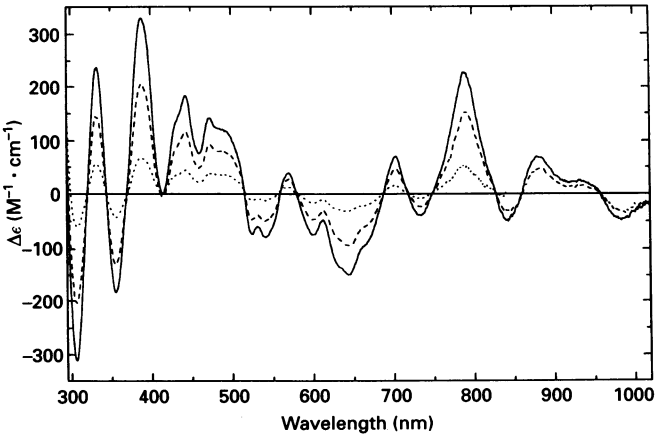

Figure 2 Low-temperature MCD spectra of $[3Fe\text{-}4Se]^{1+}$ seleno-aconitase from bovine heart

The concentration of $[3Fe\text{-}4Se]^{1+}$ clusters was 190 μM in 50% (v/v) ethanediol/0.1 M Hepes, pH 7.5. Experimental conditions of were: pathlength = 1 mm; magnetic field = 5 T. All concentrations are quoted after dilution. ——, 1.6 K; – – – –, 4.2 K; · · · ·, 14.5 K.

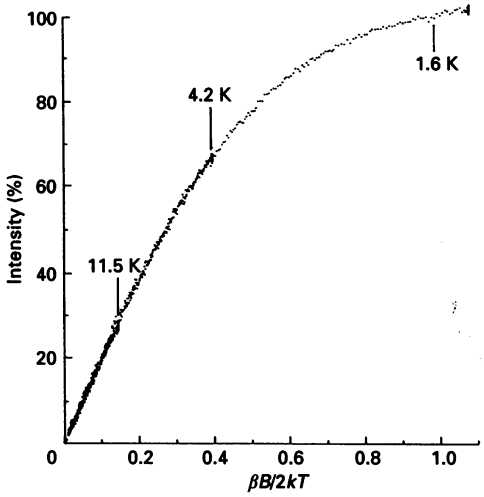

Figure 3 Magnetization curves recorded at 388 nm for [3Fe-4Se]$^{1+}$ seleno-aconitase from bovine heart

The concentration of [3Fe-4Se]$^{1+}$ clusters was 190 μM in 50% (v/v) ethanediol/0.1 M Hepes, pH 7.5. Experimental conditions: pathlength = 1 mm; magnetic field = 0–5 T. The *x*-axis label describes the normalized intensity of the MCD band, where β = Bohr magneton; B = magnetic flux density; k = Boltzman's constant; and T = absolute temperature (K). All concentrations are quoted after dilution.

RESULTS

Oxidized [3Fe-4Se]$^{1+}$ cluster

The sample was homogeneous in terms of [Fe-Se] cluster, as shown from the characteristic $g = 2.01$ EPR signal (Figure 1) of oxidized [3Fe-4Se]$^{1+}$ clusters. On integration this signal gave 0.95 ± 0.10 spin/mol at 16 K for the calculated concentration of 190 μM. This is consistent with a spin S = 1/2 ground state. The values of the ground-state *g*-tensor are shifted slightly to lower fields in 50% ethanediol solution ($g_z = 2.046$, $g_y = 1.995$, $g_x = 1.927$), when compared with the spectrum recorded in aqueous medium, for which the *g*-tensor was described by $g_z = 2.04$, $g_y = 1.985$, $g_x = 1.92$ for the spectrum simulation [22]. The main effect of selenium substitution is the greater anisotropy of the ground-state *g*-tensor. The values used to fit the corresponding EPR signal for the native [3Fe-4S]$^{1+}$ cluster are $g_1 = 2.024$, $g_2 = 2.016$ and $g_3 = 2.004$ [22]. The adventitious ferric ions derivative at $g = 4.3$ was negligible in this preparation, thus confirming its high quality.

The MCD spectrum was recorded from 295 to 1020 nm at 1.6, 4.2 and 14.5 K and 5 T (Figure 2). The inverse temperature-dependence of this spectrum indicates a paramagnetic ground state. The spectrum is very intense, with $\Delta\epsilon_{max.} = 320\ M^{-1} \cdot cm^{-1}$ at 388 nm, and overall resembles the spectrum of the sulphur-containing cluster. Magnetization curves were measured at 1.6, 4.2 and 11.5 K at several wavelengths. The curves measured at 388 nm are presented in Figure 3. The different temperature curves at each wavelength can be superimposed on each other, and the intercept value I is close to 0.5 for all transitions, thus the spin ground state is S = 1/2. I is defined as the ratio of the magnetization limit to the initial Curie slope and was introduced as a convenient index of the ground state *g*-value [37]. For an S = 1/2 ground spin state system with an isotropic *g*-tensor, I is equal to $1/g$. Analysis of transition-wavelength shifts will be presented in the next section.

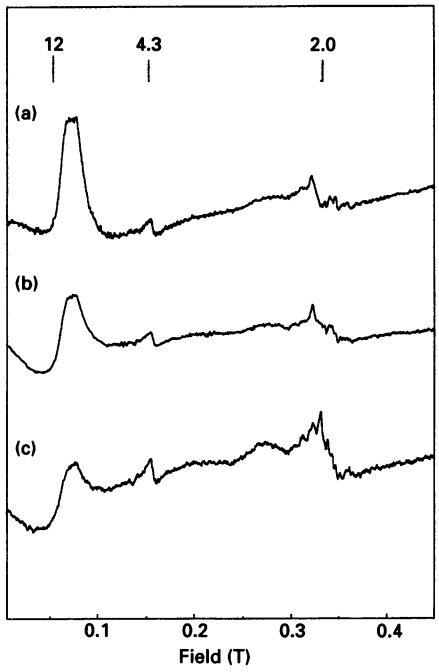

Figure 4 X-band EPR spectra of [3Fe-4Se]^{0} seleno-aconitase from bovine heart

The concentration of [3Fe-4Se]^{0} clusters was 170 μM in 50% (v/v) ethanediol/0.1 M Hepes, pH 7.5. Experimental conditions were: microwave power = 20 mW, modulation amplitude = 10 G; (**a**) temperature = 4.2 K; gain = 1×10^5; (**b**) temperature = 9 K, gain = 1.6×10^5; (**c**) temperature = 20 K, gain = 5×10^5. All concentrations are quoted after dilution. Effective *g*-values are indicated on the spectra.

Reduced [3Fe-4Se]^{0} cluster

Low-temperature EPR spectra of the [3Fe-4Se]^{0} sample are presented in Figure 4. The most prominent feature is the broad low-field absorption trough followed by a peak centred around 0.06 T. At 4.2 K and 20 mW microwave power (Figure 4,

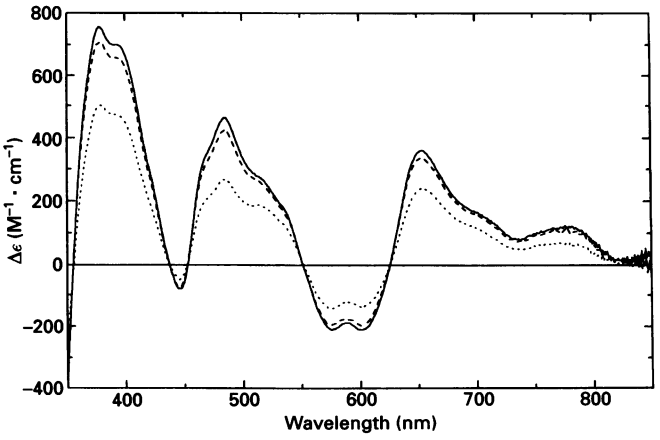

Figure 5 Low-temperature MCD spectra of [3Fe-4Se]^{0} seleno-aconitase from bovine heart

The concentration of [3Fe-4Se]^{0} clusters was 170 μM in 50% (v/v) ethanediol/0.1 M Hepes, pH 7.5. Experimental conditions were: pathlength = 1 mm; magnetic field = 5 T. All concentrations are quoted after dilution. ——, 1.6 K; – – – –, 4.2 K; · · · ·, 10 K.

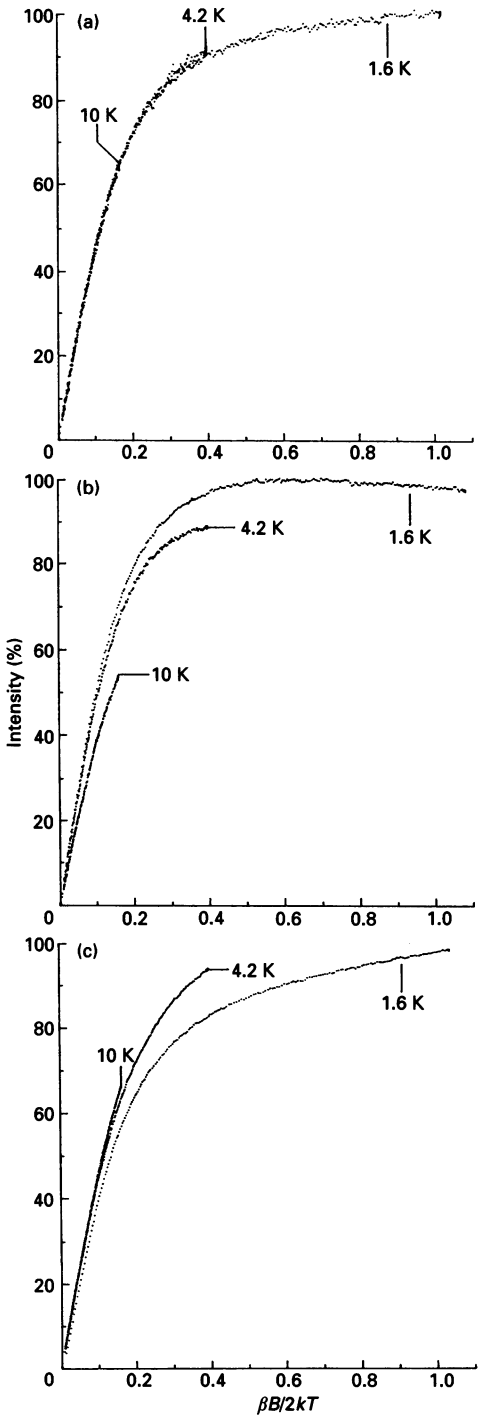

Figure 6 Magnetization curves recorded at (a) 603 nm, (b) 485 nm and (c) 395 nm for [3Fe-4Se]$^{1+}$ seleno-aconitase from bovine heart

The concentration of [3Fe-4Se]$^{1+}$ clusters was 170 μM in 50% (v/v) ethanediol/0.1 M Hepes, pH 7.5. Experimental conditions were: pathlength = 1 mm; magnetic field = 0–5 T. All concentrations are quoted after dilution.

spectrum a), this signal is very intense for this type of $g = 12$ signal, which is formally a spin-forbidden transition in the perpendicular-mode EPR spectrometer. At higher temperatures (Figure 4, spectra b and c) the shape of the peak becomes more asymmetrical, with the trough on the low-field side of the resonance becoming more prominent. At 20 K the peak is significantly decreased in intensity and broadened. Other minor signals are also observed. A very small contribution from adventitious ferric iron is indicated by the derivative at $g \approx 4.3$, and a six-line signal around $g \approx 2$, increasing with temperature, probably arises from trace manganese impurities.

The corresponding MCD spectra, presented in Figure 5, were recorded at 1.6, 4.2 and 10 K and 5 T, from 340 to 850 nm. Again, this spectrum is very intense below 750 nm, with $\Delta\epsilon_{max.} \approx 750\ M^{-1}\cdot cm^{-1}$ at 377 nm. Other major positive bands with $\Delta\epsilon \approx 400\ M^{-1}\cdot cm^{-1}$ occur at 485 and 603 nm, and two troughs with $\Delta\epsilon \approx -200\ M^{-1}\cdot cm^{-1}$ occur at 575 and 653 nm. Above 750 nm, the transitions have positive intensities with an absorption coefficient of the order of $50\ M^{-1}\cdot cm^{-1}$. A full set of magnetization curves was recorded at 1.6, 4.2 and 10 K (Figures 6a–6c). The temperature-dependence of the spectrum indicates a paramagnetic ground state. The sets of curves are all different from one another, but can be grouped into three subsets. The 603 nm band has the steepest initial slope, with the three temperature curves overlaying each other (Figure 6a). The 485 nm (and the 785 nm) band has nested curves, with the 10 K curve below the 1.6 K and 4.2 K curves (Figure 6b). The remaining transitions have opposite nesting, with the 10 K curve either slightly above or overlaying the 4.2 K curve, as shown by the curves recorded at 395 nm (Figure 6c).

DISCUSSION

Oxidized [3Fe-4Se]$^{1+}$ cluster

The EPR results for [3Fe-4Se]$^{1+}$ seleno-aconitase indicate that the spin ground state was paramagnetic, $S = 1/2$. The $g = 2.01$ signal originating from this species is of a new type, being more rhombic than the classical $g = 2.01$ signals from [3Fe-4Se]$^{1+}$ clusters. This increase in rhombicity was reflected in the parameters used for the spectral simulation, the g-tensor for the oxidized Se cluster being described by $g_x = 1.92$, $g_y = 1.985$, $g_z = 2.04$, as opposed to $g_x = 2.004$, $g_y = 2.016$, $g_z = 2.024$ for the native [3Fe-4S]$^{1+}$ cluster [22]. Hence, incorporation of selenium into the core of the cluster perturbed its electronic structure, increasing the molecular axis g-value anisotropy (Δg_{xy} and g_{yz} are now almost equal) away from the near-axial case of the sulphur cluster ($\Delta g_{xy} > \Delta g_{yz}$).

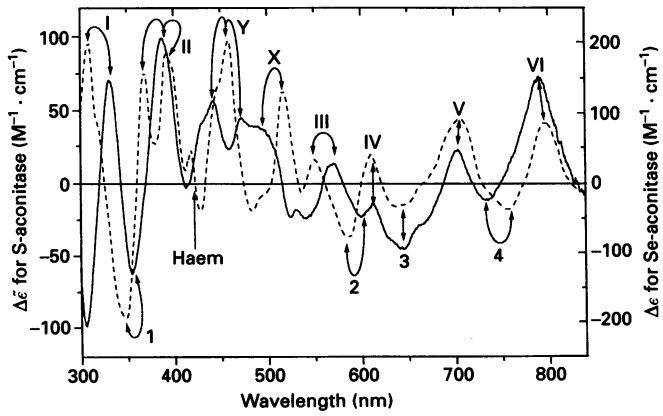

Figure 7 Comparison of the MCD spectra of [3Fe-4Se]$^{1+}$ seleno-aconitase (——) and [3Fe-4S]$^{1+}$ aconitase from bovine heart at pH 7.5 (Figure 1 from ref [37]) (– – – –)

The temperature was 4.2 K and the magnetic field 5 T.

Table 1 Transition wavelength shifts of the [3Fe-4Se]$^{1+}$ cluster on selenium substitution

The numbers before each transition refer to the numbers on Figure 7.

	Region (a) (300–420 nm)	Region (b) (420–550 nm)	Region (c) (550–840 nm)
Peak wavelength shift	(II) 311 → 332 (I) 311 → 332 (II) 370 → 387 389 → 387	(X) 519 → 471 (X) 519 → 497 (Y) 458 → 439 458 → 471	(IV) 550 → 120 (III) 550 → 570 (IV) 611 → 611 (V) 701 → 701 (VI) 795 → 789
Trough wavelength shift	(1) 347 → 354		(2) 586 → 601 (3) 643 → 643 (4) 754 → 732
General trend	Red shift, ≈ 20 nm	Both red and blue shifts	Invariant (600–720 nm) Blue shift (720–840 nm)

Double integration of this signal yielded approx. 1 spin/mol. Therefore are no significant proportions of the seleno-cluster population with $S > 1/2$, as opposed to the situation arising in certain [4Fe-4Se]$^{1+}$ clusters [21].

MCD spectroscopy confirms these results. The superimposable magnetization curves point to a homogeneous paramagnetic population with spin ground state $S = 1/2, g_o = 2.0$. The increase in intensity of this spectrum, compared with its sulphur counterpart, is at least twofold (e.g. $\Delta\epsilon \approx 150$–$300\ M^{-1}\cdot cm^{-1}$ in the 300–500 nm region for [3Fe-4Se]$^{1+}$, $\Delta\epsilon \approx 75$–$150\ M^{-1}\cdot cm^{-1}$ for [3Fe-4S]$^{1+}$). Consequently, the effect of the fourfold increase in the spin–orbit coupling constant of selenium is responsible for a twofold increase in MCD intensity.

The transition shifts occurring on selenium substitution were analysed by comparing the MCD spectra of the [3Fe-4S]$^{1+}$ and [3Fe-4Se]$^{1+}$ clusters (Figure 7). There is a good general peak-to-peak correlation between these two spectra, although in the regions where the larger shifts are expected (the higher-energy part of the spectrum) it is sometimes difficult to assign certain correspondences, as unresolved shoulders and peaks in the sulphur spectrum might lead to 'new' or on the other hand 'missing' transitions in the selenium spectrum. A list of wavelength shifts based on this assignment is given in Table 1. The spectrum can be partitioned into three arbitrary regions. In region (a), from 300 to 420 nm, the spectrum appears to be red-shifted (bathochromic shift) by an average of 20 nm [e.g. (I) 311 nm → 332 nm]. In region (c), from 550 to 840 nm, most transitions are left unchanged [e.g. (V) 701 nm], with others above 720 nm blue-shifted by a maximum of 10 nm. In region (b), from 420 to 550 nm, the situation is the most unclear. For example band (Y), which comprises more than one transition as shown by the shoulders on both sides of the main peak, appears to have split into at least two new peaks, one blue-shifted (458 → 439 nm), the other red-shifted (458 → 471 nm).

These observations can help to distinguish between different types of transitions in the UV/visible MCD spectrum. The transitions can be assigned as ligand-to-metal charge-transfer, either S from a terminal cysteinyl ligand, or Se from the inorganic Se^{2-} ions of the core. As only the inorganic ligands were substituted in the protein, the observed wavelength shifts must therefore be attributed to inorganic $Se^{2-} \rightarrow$ Fe charge-transfer transitions. The bands of region (a) appear to originate from ligand S(e) → metal charge-transfer transitions, as it was observed earlier that selenium substitution had the general effect of

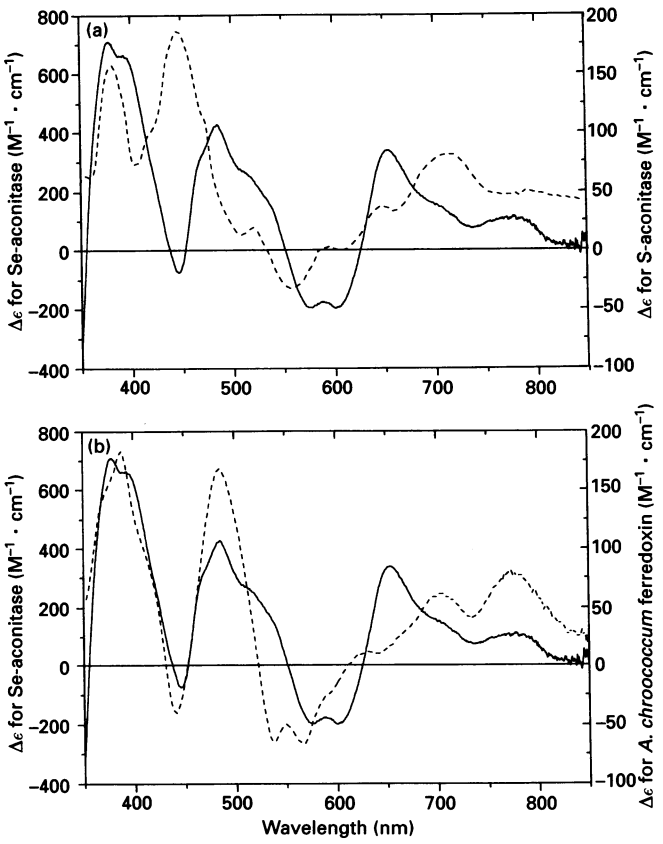

Figure 8 (a) Comparison of the MCD spectra of [3Fe-4Se]^0 seleno-aconitase (——) and [3Fe-4S]^0 aconitase from bovine heart at pH 7.5 (Figure 6 from ref. [38]) (– – – –), and (b) comparison of the MCD spectra of [3Fe-4Se]^0 seleno-aconitase (——) and [3Fe-4S]^0 from *Azotobacter chroococcum* ferredoxin at pH 6.3 (Figure 1 from ref. [39]) (– – – –)

The temperature was 4.2 K and the magnetic field 5 T.

decreasing charge-transfer energies [19,20], this producing bathochromic shifts as observed here. The fact that these red shifts are localized in the high-energy part of the spectrum also supports this proposition. On the other hand, only small or negligible shifts are observed for the rest of the spectrum, which must therefore comprise principally cysteinyl S → Fe charge-transfer transitions and other d → d transitions associated with the metal core.

Reduced [3Fe-4Se]^0 cluster

The EPR spectrum of the reduced cluster gave rise to a very prominent low-field resonance with $g_{eff.} \approx 9$. This signal is indicative of a paramagnetic species with an integer ground spin state. It was observed by Mössbauer spectroscopy that the electronic structures of [3Fe-4S]^0 and [3Fe-4Se]^0 were very similar [22], and as the ground spin state of the reduced sulphur cluster is $S = 2$ [6,38], this ground site is also tentatively assigned to the reduced selenium cluster. Although EPR results enable us to assign $S \geqslant 1$, values other than 2 are very unlikely as they would require a new coupling scheme between the iron atoms or population of an excited state. Either solution would necessitate that noticeable differences in the Mössbauer parameters of the selenium cluster be observed.

The corresponding MCD spectrum of the selenium cluster is

very intense ($\Delta\epsilon_{max.} \approx 750\ M^{-1} \cdot cm^{-1}$), being nearly four times more intense than the sulphur cluster spectrum [38], as shown in Figure 8. The magnetization curves support a ground state assignment $S \geqslant 1$. The MCD magnetization curves shown in Figure 6 are not identical with those of the [3Fe-4S]^0 analogue and are not analysed in a simple way by the method of intercepts [37].

A comparison between the MCD spectra of [3Fe-4S]^0 and [3Fe-4Se]^0 clusters (Figure 8a) shows substantial energy shifts between peaks of the same sign throughout the spectrum. This is at first sight rather surprising given the close correspondence between the peaks in the oxidized form of the cluster. However, the [3Fe-4S]^0 cluster can exist in a protonated state as was first reported for the case of ferredoxin (Fd)I from *A. chroococcum* [39], and subsequently confirmed for *A. vinelandii* FdI [40,41]. The protonation of the [3Fe-4S]^0 cluster leads to a remarkable change in the MCD spectrum. In Figure 8(b) a comparison is made between the MCD spectra of the [3Fe-4Se]^0 cluster and the protonated state of the [3Fe-4S]^0 of *A. chroococcum* FdI. In the 350–600 nm region a one-to-one correspondence between the individual MCD C-terms is seen. This suggests that the [3Fe-4Se]^0 cluster may be protonated at pH 7.5. The pK_a value for the protonation of the cluster in *A. chroococcum* and *A. vinelandii* FdI is 7.8 [42,43]. In a study of the MCD of bovine heart aconitase, no protonation could be detected between pH 6.4 and 8.9 [44]. However, a recent electrochemical study of aconitase gave evidence for a pH-dependence of the [3Fe-4S]$^{1+/0}$ cluster redox potential, and concluded that there is either a one or two H^+ ion uptake involved on this reduction step [45]. A pK_a value was not determined, neither was any spectroscopic evidence presented for a protonation process directly at the cluster. We are currently re-investigating with spectroscopic methods the protonation of the [3Fe-4S]^0 cluster in aconitase.

Hence a comparison of the wavelength shifts between the sulphur and selenium forms of the reduced three-iron cluster cannot be made conclusively until the question of the protonation state is resolved definitely. The comparison drawn in Figure 8(b), based on the assumption of protonation of the cluster, indicates that the transitions in the 400–500 nm region are relatively unaffected by a change to the selenium form and could be assigned to thiolate-to-iron charge transfer. The transitions lying in the range between 500 and 800 nm would therefore have considerably higher selenium-to-iron charge-transfer character. However, the intra-iron d–d transitions will experience increased spin–orbit coupling mixing with the charge-transfer states and may also play a prominent part.

This work was supported by grants from the U.K. Engineering and Physical Sciences Research Council (to A.J.T.) and from the U.S. National Institute of Health (GM34812) (to H.B.).

REFERENCES

1 Emptage, M. H., Kent, T. A., Huynh, B. H., Rawlings, J., Orme-Johnson, W. H. and Münck, E. (1980) J. Biol. Chem. **255**, 1793–1796
2 Papaefthymiou, V., Girerd, J. J., Moura, I., Moura, J. J. G. and Münck, E. (1987) J. Am. Chem. Soc. **109**, 4703–4710
3 Huynh, B. H., Moura, J. J. G., Moura, I. et al. (1980) J. Biol. Chem. **255**, 3242–3244
4 Gayda, J. B., Bertrand, P., Theodule, F. X. and Moura, J. J. G. (1982) J. Chem. Phys. **77**, 3387–3391
5 Hagen, W. R., Dunham, W. R., Johnson, M. K. and Fee, J. A. (1985) Biochim. Biophys. Acta **828**, 369–374
6 Thomson, A. J., Robinson, A. E., Johnson, M. K. et al. (1981) Biochim. Biophys. Acta **670**, 93–100
7 Day, E. P., Peterson, J., Bonvoisin, J. J., Moura, I. and Moura, J. J. G. (1988) J. Biol. Chem. **263**, 3684–3689
8 Johnson, M. K., Hare, J. W., Spiro, T. G., Moura, J. J. G., Xavier, A. V. and LeGall, J. J. (1981) J. Biol. Chem. **256**, 9806–9808
9 Johnson, M. K., Czernuszewicz, R. S., Spiro, T. G., Fee, J. A. and Sweeney, W. V. (1983) J. Am. Chem. Soc. **105**, 6671–6678
10 Kilpatrick, L., Kennedy, M. C., Beinert, H., Czernuszewicz, R. S., Qiu, D. and Spiro, T. G. (1994) J. Am. Chem. Soc. **116**, 4053–4061
11 Kent, T. A., Huynh, B. H. and Münck, E. (1980) Proc. Natl. Acad. Sci. U.S.A. **77**, 6574–6576
12 Tsibris, J. C. M., Namtvedt, M. J. and Gunsalus, I. C. (1968) Biochem. Biophys. Res. Commun. **30**, 323–327
13 Moulis, J.-M. and Meyer, J. (1982) Biochemistry **21**, 4761–4771
14 Cotton, F. A. and Wilkinson, G. (1980) Advanced Inorganic Chemistry, 4th edn., Wiley, New York
15 Odom, J. D. (1983) Struct. Bond. **54**, 1–26
16 Malkin, R. and Rabinowitz, J. C. (1966) Biochem. Biophys. Res. Commun. **23**, 822–827
17 Hong, J. S. and Rabinowitz, J. C. (1970) J. Biol. Chem. **245**, 6574–6581
18 Orme-Johnson, W. H., Hansen, R. E., Beinert, H., Tsibris, J. C. M., Bartholomaus, R. C. and Gunsalus, I. C. (1968) Proc. Natl. Acad. Sci. U.S.A. **60**, 368–372
19 Bobrik, M. A., Laskowski, E. J., Johnson, R. W. et al. (1978) Inorg. Chem. **17**, 1402–1410
20 Yu, S., Papaefthymiou, G. C. and Holm, R. H. (1991) Inorg. Chem. **30**, 3476–3485
21 Meyer, J., Moulis, J.-M., Gaillard, J. and Lutz, M. (1992) Adv. Inorg. Chem. **38**, 74–115
22 Surerus, K. K., Kennedy, M. C., Beinert, H. and Münck, E. (1989) Proc. Natl. Acad. Sci. U.S.A. **86**, 9846–9850
23 He, S. H., Texeira, M., LeGall, J. et al. (1989) J. Biol. Chem. **264**, 2678–2682
24 Mullen, G. P., Dunlap, R. B. and Odom, J. D. (1985) J. Am. Chem. Soc. **107**, 7187–7189
25 Johnson, M. K., Thomson, A. J., Robinson, A. E. and Smith, B. E. (1981) Biochim. Biophys. Acta **671**, 61–70
26 Maclean, P. A., Papaefthymiou, V., Orme-Johnson, W. H. and Münck, E. (1987) J. Biol. Chem. **262**, 12900–12903
27 Hagen, W. R., Eady, R. R., Dunham, W. R. and Haaker, H. (1985) FEBS Lett. **189**, 250–254
28 George, S. J., Armstrong, F. A., Hatchikian, E. C. and Thomson, A. J. (1989) Biochem. J. **264**, 275–284
29 Conover, R. C., Kowal, A. T., Fu, W. et al. (1990) J. Biol. Chem. **265**, 8533–8541
30 Õnate, Y. A., Vollmer, S. J., Switzer, R. L. and Johnson, M. K. (1989) J. Biol. Chem. **264**, 18386–18391
31 Carney, M. J., Papaefthymiou, G. C., Spartalian, K., Frankel, R. B. and Holm, R. H. (1988) J. Am. Chem. Soc. **110**, 6084–6095
32 George, S. J., Thomson, A. J., Crabtree, D. E., Meyer, J. and Moulis, J.-M. (1991) New J. Chem. **15**, 455–465
33 Kennedy, M. C. and Beinert, H. (1988) J. Biol. Chem. **263**, 8194–8198
34 Beinert, H. and Kennedy, M. C. (1989) Eur. J. Biochem. **186**, 5–15
35 Aasa, R. and Vänngård, T. (1975) J. Magn. Reson. **19**, 308–315
36 Thomson, A. J., Cheesman, M. R. and George, S. J. (1993) Methods Enzymol. **226**, 199–231
37 Thomson, A. J. and Johnson, M. K. (1980) Biochem. J. **191**, 411–420
38 Johnson, M. K., Thomson, A. J., Richards, A. J. M. et al. (1984) J. Biol. Chem. **259**, 2274–2282
39 George, S. J. G., Richards, A. J. M., Thomson, A. J. and Yates, G. M. (1984) Biochem. J. **224**, 247–251
40 Johnson, M. K., Bennett, D. E., Fee, J. A. and Sweeney, J. W. (1987) Biochim. Biophys. Acta **911**, 81–94
41 Stephens, P. J., Jensen, G. M., Devlin, F. J. et al. (1991) Biochemistry **30**, 3200–3209
42 Armstrong, F. A., George, S. J. G., Thomson, A. J. and Yates, G. M. (1988) FEBS Lett. **234**, 107–110
43 Iismaa, S. E., Vásquez, A. E., Jensen, G. M. et al. (1991) J. Biol. Chem. **266**, 21563–21571
44 Richards, A. J. M. (1986) Ph.D. Thesis, University of East Anglia
45 Tong, J. and Feinberg, B. A. (1994) J. Biol. Chem. **269**, 24920–24927

Received 10 April 1995; accepted 1 June 1995